UCID-20174

Electrochemical Determination of the Corrosion Behavior of Candidate Alloys Proposed for Containment of High Level Nuclear Waste in Tuff

Robert S. Glass
George E. Overturf
Robert E. Garrison
R. Daniel McCright

June 1984

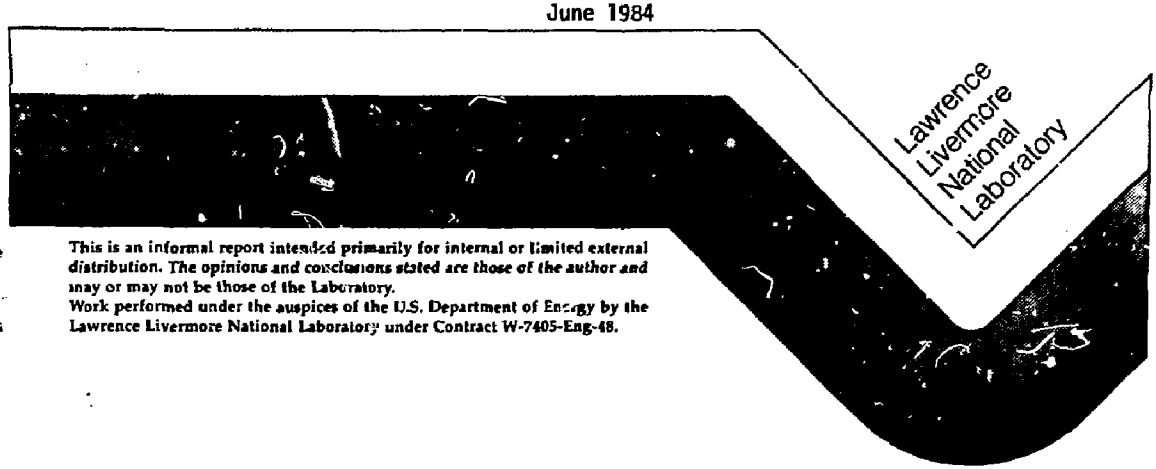

Electrochemical Determination of the Corrosion Behavior of Candidate Alloys Proposed for Containment of High Level Nuclear Waste in Tuff

Robert S. Glass, George E. Overturf,
Robert E. Garrison, and R. Daniel McCright

UCID--20174

DE85 001768

June 18, 1984

ABSTRACT

*Long-term geological disposal of nuclear waste requires corrosion-*resistant canister materials for encapsulation. Several austenitic stainless steels are under consideration for such purposes for the disposal of high-level waste at the candidate repository site located at Yucca Mountain, Nevada. With regard to corrosion considerations, a worst case scenario at this prospective repository location would result from the intrusion of vadose water. This preliminary study focuses on the electrochemical and corrosion behavior of the candidate canister materials under worst-case repository environments. Electrochemical parameters related to localized attack (e.g., pitting potentials) and the electrochemical corrosion rates have been examined.

Introduction

Lawrence Livermore National Laboratory (LLNL) is responsible for high-level nuclear waste package development for the Nevada Nuclear Waste Storage Investigations project as a part of the Department of Energy's Civilian Radioactive Waste Management (CRWM) Program. The waste package

effort at LLNL is developing multi-barriered packages for safe, permanent disposal in a repository in the unsaturated zone at Yucca Mountain. The corrosion-resistant austenitic stainless steels AISI 304L, 316L, 321, and 347 and the high-nickel alloy 825 are under investigation for use as canister materials in the encapsulation of nuclear waste materials (1). The canister must have sufficient corrosion resistance to survive for 300-1000 years in the repository environment. Repository environmental considerations include the potentially aggressive situation where vadose water intrudes into the repository and contacts the emplaced stainless steel canisters. The repository horizon would be located in welded tuff above the static water table at Yucca Mountain. Some water could percolate down through fractures in the rock and enter the horizon of the repository. The environment surrounding the waste canisters for much of the containment period is therefore expected to be air and water vapor (steam). A potentially worst-case environment would be partial to complete inundation with vadose water when the radioactive waste has decayed appreciably and the canisters have cooled to below 95°C surface temperature (the boiling point of water at the repository elevation).

As a result of their widespread structural use, the electrochemical and general corrosion properties of stainless steels have been extensively investigated (2-6). Localized forms of corrosion such as pitting and crevice corrosion, although again extensively investigated, require additional work to resolve outstanding issues. Different environments impose various constraints on the selection of the appropriate austenitic stainless steel for the desired application.

The purpose of this preliminary study was to survey the electrochemical parameters relating to general corrosion (e.g., corrosion potential, corrosion current) and to localized corrosion (e.g., pitting potential, protection

potential). These parameters were examined for the candidate steels in water characteristic of the prospective repository site. The data reported here represent the results to date and it is to be stressed that much work remains to be done. A more detailed analysis of the significance of the electrochemical results presented here is underway. The mechanisms of localized attack as well as the role of thermal oxide films in corrosion resistance needs to be better understood for the prospective environmental conditions. In addition, the effect of ionizing radiation on the chemical environment surrounding the waste canisters needs to be evaluated in light of possible changes in corrosion resistance.

Experimental Considerations

The water used in this experimental work was obtained from the J-13 well at the Nevada Test Site. While water samples have not yet been obtained from the location of the prospective repository in Yucca Mountain, near-by well J-13 produces water which has flowed through Topopah Spring member where it lies at lower elevation and is in the saturated zone. The water from the J-13 well is taken as a reference water in the repository horizon. The chemical composition of tuff-conditioned J-13 water is given in Table 1.

The small amounts of the anions such as Cl^- suggest a relatively benign environment with regard to the expected performance of the candidate stainless steel. When additions of Cl^- were intentionally made to solution, analytical grade NaCl was used. The metal samples used were obtained from Metal Samples, Inc. and were used in the mill-annealed condition.

The electrochemical cell used consisted of a one l flask with inlets for the working, counter, and reference electrodes. The reference electrode used was in all cases a saturated calomel electrode (S.C.E.). All potentials quoted

in the paper were corrected to reference an S.C.E. at 25°C. Graphite rods were used as the counter electrodes. Unless otherwise stated, the solutions were air-saturated and static. When deaeration was used, ultra-high purity argon was used to bubble the solution throughout the experiment.

The working electrodes employed usually consisted of discs 1 cm^2 in area which were masked off by neoprene o-rings in a commercial gasket electrode holder (Princeton Applied Research). In some cases, a 5 cm^2 cylinder of the material of interest was used. Generally, the electrodes were pretreated by polishing to 400 grit SiC and rinsing with DI water. The ASTM specifications for elemental ranges for the alloys used in this work are given in Table 2. The actual analyses for the alloys used are listed in Table 3.

Unless otherwise stated, the anodic polarization curves were obtained potentiodynamically at a 1 mV/s scan rate. The electrochemical parameters E_{corr}, E_{pit} and E_{prot} were determined at this scan rate. The electrochemical corrosion rates obtained by Tafel extrapolation and linear polarization resistance (L.P.R.) were also obtained at this scan rate. Electrochemical data was generally obtained with the aid of a EG&G Princeton Applied Research Model 350A Corrosion Measurement Console. In some cases, the polarization curves were obtained using an EG&G Princeton Applied Research Model 173 potentiostat in combination with a model 175 function generator and 176 i/E converter.

Description of Electrochemical Techniques

The techniques used in the present study to extract electrochemical parameters include cyclic anodic polarization, Tafel extrapolation and linear polarization resistance (LPR). Excellent descriptions of these techniques are given in the literature (2-4, 7, 8), and only a brief recounting is given here.

Cyclic anodic polarization curves are obtained by anodically scanning the sample (working electrode) to enforced potentials anodic to the corrosion potential (E_{corr}), then reversing the direction of the scan back to more negative valves. Current flowing through the working electrode/counter electrode couple is continuously monitored during the scan. Such a scan, whose potential waveform is triangular, yields electrochemical values of interest such as the pitting potential (E_{pit}) and the protection potential (E_{prot}). The pitting potential is the potential above which pits spontaneously initiate and grow. The protection potential is the potential below which previously initiated pits repassivate and no new pits form. At potentials between the pitting and protection potential, new pits are not initiated, but any previously initiated pits continue to grow. The values of the pitting and protection potential relative to the corrosion potential are indicative of the pitting susceptibility of the tested alloy in the tested environment. It is to be noted that the values for E_{pit}, E_{prot} and E_{corr} are in many cases dependent upon the particular electrochemical technique employed. In this study, the potentiodynamic method was used in which the potential is continually scanned anodically with time. For consistency, the technique was used throughout this screening study for all the alloys. Other techniques, such as potentiostatic methods, are currently being used to investigate in more detail the values of E_{pit}, E_{prot}, etc.

An "electrochemical" corrosion rate can be determined either by Tafel extrapolation or LPR. In LPR, a linear polarization measurement is performed in the potential range close to, and on either side of the corrosion potential (e.g., ± 10 mv). In this region, the current-potential relationship can be linearized and from plots of i-E one can determine a " polarization resistance." With the additional knowledge of some fundamental

electrochemical parameters (Tafel coefficients), a corresponding electrochemical corrosion rate (in $\mu A/cm^2$) can be calculated. This is then easily converted into a corrosion rate in mils-per-year through use of Faraday's Law. The interested reader is directed to the references above for a detailed description of the theory behind this technique.

Tafel extrapolations can also be used to calculate corrosion rates. In this method, one linearly scans the potential region to a few hundred millivolts anodic and cathodic of the corrosion potential. Plots are then made of the potential (or potential relative to the corrosion potential, e.g., overpotential) vs the logarithm of the current. By extrapolation of the linear segments of either anodic or cathodic branches back to the measured corrosion potential, the corrosion current can be obtained. Again, the corrosion current can be easily converted into a corrosion penetration rate. The interested reader is again directed to the literature references given above for a detailed description of the theory of this technique

Results and Discussion

General Electrochemistry

Most of the electrochemical work to date has been performed in the relatively benign J-13 well water, and in environments somewhat more aggressive than this. The addition of chloride ion will make the environment more aggressive towards austenitic stainless steels (2-4), and chloride ion has been purposely added in some experiments.

A typical anodic polarization curve is shown in Fig. 1. The curve shown here is for 304L in J-13 well water at 90°C. This curve displays features common to all polarization curves obtained in the J-13 well water environment. In this figure, the electrochemical parameters E_{corr}, E_{pit}, E_{prot}, and the passive current region are identified. Scanning anodically

from E_{corr}, 304L remains passive until the pitting potential is reached. This characteristic potential, which is influenced largely by such parameters as temperature and chloride ion concentration, is marked by a large increase (several orders of magnitude) in the anodic current density. The exact potentials are influenced by the surface pretreatment and the particular electrochemical method employed (2,9). The closer E_{pit} is to E_{corr}, the greater susceptibility to pitting may result from increase in the oxidizing potential of the media, which would shift E_{corr} to more positive values.

From plots like those in Fig. 1, tabulations of electrochemical parameters for some of the prospective canister materials have been made. Figure 2 lists values of E_{corr}, E_{pit}, E_{prot}, and E_{pit}-E_{prot} for 304L in J-13 well water at various temperatures. The parameter E_{pit}-E_{prot} has been used previously to "rank" alloys in terms of crevice corrosion resistance (10). In the above study, the value of E_{pit}-E_{prot} determined in aerated 3.5% NaCl at 25°C correlated very well with the natural crevice corrosion weight loss in seawater after several years immersion for the austenitic stainless steels investigated. As the value of E_{pit}-E_{prot} becomes larger, the resistance to crevice corrosion decreases. Also, greater difficulty in repassivating growing pits is indicated by larger values of E_{pit}-E_{prot}.

The data shown for 304L in Fig. 2 indicate no clear temperature dependence for E_{corr} in the range of 60 to 90°C. That J-13 well water is relatively benign may account for this. In harsher environments, one generally expects a more dramatic shift of E_{corr} to more negative potentials with increasing temperature which in most cases indicates a loss of passive oxide film stability, e.g., film thinning. For E_{pit} values, again, no significant temperature dependence is observed. A shift in E_{pit} to more negative potentials can, in some cases, be an indication of greater

susceptibility to pitting corrosion, and is commonly observed as the temperature is increased (2-4). For the case at hand, the values of E_{pit} are sufficiently removed from E_{corr} such that pitting will not occur. The value of E_{pit}-E_{prot} generally shows a tendency to adopt larger values with increasing temperature in agreement with the negative temperature dependence of E_{prot}. This could indicate a slightly greater susceptibility to crevice attack. Further experiments to confirm this will need to be performed. At 60°C and 70°C, the E_{prot} values are essentially equivalent to the E_{pit} values. This indicates that pits can be repassivated at the same potential at which they initiate.

Electrochemical parameters for 316L and I-825 equivalent to those for 304L in J-13 well water are presented in Figures 3 and 4, respectively. Again, there is no strong dependence of the corrosion potential on temperature in this environment, at least in the temperature range of 50-90°C. The values for E_{corr} for 316L and I-825 are fairly close, and generally more positive than those for 304L. The observation of more noble corrosion potentials for the more highly alloyed materials may be related to the well-acknowledged roles of Mo and Ni as passivating agents. These alloying constituents may shift the corrosion potential positive by creating more stable passive films or by decreasing the overvoltage for the cathodic half-reaction in the overall corrosion process.

A stronger negative temperature dependence of E_{pit} values for 316L and I-825 was observed than for 304L. The values of E_{pit} for 316L are generally more positive than those for 304L which indicates a lower susceptibility to pitting in this environment. This again may be related to the well-known role of the alloying consistent Mo in increasing the pitting resistance in stainless steels (2-4). The alloy I-825, on the other hand, shows values of

E_{pit} lower than those for 304L at 80° and 90°C. In any case, for all of the alloys, 304L, 316L, and I-825, the pitting potential is significantly removed (positive) from E_{corr} such that in the absence of a large change in solution chemistry to more oxidizing conditions, no spontaneous pitting of any of these alloys in this environment is likely to occur.

No statistically significant trends in E_{prot} or in E_{pit}-E_{prot} are noted for either 316L or I-825. For all of the alloys 304L, 316L, and I-825, the small values of E_{pit}-E_{prot} indicate that it is relatively easy to electrochemically repassivate growing pits.

In-situ corrosion testing is performed by sandwiching flat metal specimens between ribbed Teflon washers. All of the alloys examined in this work (304L, 316L, 321, 347, and I-825) showed some "preferential attack" in the crevices under the Teflon washers. At the one year time period, however, in J-13 well water at temperatures ranging between 50° and 100°C, the attack was very minor. Many samples showed what would be better described as a "stain" rather than having any real significant depth of penetration (15).

It is to be noted that while the electrochemical parameters of E_{pit}, E_{prot} and other general i-E relationships were determined through the potentiodynamic technique, more sophisticated electrochemical techniques exist (2,9,11). The values reported in this work should, therefore, be considered as preliminary in the sense that they were evaluated as part of a general screening study. More powerful and more time consuming electrochemical techniques exist for the examination of localized corrosion such as the pit-propagation rate method used in evaluating pitting phenomena (9).

Surface preparation also plays a role in determining potential measurements, both the precision and reliability, particularly for E_{corr}. An in-depth study evaluating this factor for austenitic steels is now underway.

Chloride ion acts as a very aggressive anion with regard to localized corrosion (pitting and crevice attack) of stainless steels (2-4). It is possible, due to evaporation and radiolysis effects, that J-13 well water may "concentrate" in an actual repository environment. To evaluate the effect of increased Cl^- levels, this anion was purposely added to J-13 well water. Further experiments are currently underway using "concentrated" J-13 (by boil-down) to evaluate effects on candidate alloy electrochemistry and will be reported in a future report.

Preliminary data for a solution ten times more concentrated than J-13 indicate no significant effect on the electrochemical corrosion behavior of 316L (with respect to J-13). Apparently the increase in beneficial effects associated with ions such as NO_3^- and HCO_3^- offset effects due to increase in Cl^- concentration. The beneficial effects of certain anions on mitigating the detrimental effects of chloride has been discussed by Smialowska (12). The electrochemical effects on 316L in deaerated J-13 well water at 90°C containing an additional 100 ppm and 1000 ppm Cl^- are shown in the anodic polarization curves in Figs. 5 and 6, respectively. In Fig. 5, E_{corr} was -0.190 V. Upon scanning to more positive potentials from this point, a passive region exists until one gets to approximately 0.27 V at which point the current begins to increase rapidly with potential. This point can be equated with the pitting potential. On the other hand, in Fig. 6 with 1000 ppm Cl^-, there is no clear breakaway point in the current-potential curve and pits may begin to nucleate at potentials very close to the corrosion potential, which is at -0.23V. However, significant pitting will not occur until potentials more positive than approximately 0.08 V are reached.

The effect of increased Cl^- concentration is apparent in the increased susceptibility to pitting which manifests itself by the proximity of E_{pit} to E_{corr} and in the magnitudes of the current densities.

Figure 7 displays the relationship between the electrochemical parameters E_{corr} and E_{pit} for 304L in J-13 well water at 90°C with varying concentrations of NaCl. The general trend for both of these values is to become more negative with increasing chloride ion concentration. It is also observed that as the concentration of chloride (i.e., NaCl) is increased, the values of E_{pit} approach more closely the values of E_{corr}. This indicates a greater susceptibility to pitting as small changes in solution oxidation potential can shift 304L into the pitting regime (e.g., compare Figs. 5 and 6). Sharp drops in E_{pit} are noted in going from 25 to 50 ppm NaCl and from 50 to 1000 ppm NaCl. At the other extremes (0 to 25 and 1000 to 30,000 ppm NaCl) less abrupt changes are noted.

The electrochemical parameters of interest for 304L in J-13 well water with 75 ppm and 1000 ppm NaCl added as a function of temperature are shown in Figs. 8 and 9, respectively. For the case of 75 ppm NaCl, a negative temperature dependence of E_{corr} and E_{pit} is noted, as expected. In the temperature range investigated, E_{pit} is far removed from E_{corr} such that pitting shoule not be a problem in this environment.

For the case of J-13 well water containing 1000 ppm NaCl shown in Fig. 9, several points are made. First, it is noted that there exists no strong temperature dependence of either E_{corr} or E_{prot} in this environment. The values for E_{corr} are more negative than those in the case of 75 ppm NaCl, which is as expected given the harsher conditions. The value of E_{corr} at 60° is curious and deserves re-examination. E_{pit} values, also in accordance with the harsher environment, are much more negative than those of the 75 ppm NaCl case, and show a negative temperature dependence. The proximity of E_{corr} and E_{pit} values indicate a higher susceptibility to pitting than was the case for 75 ppm NaCl. The values for E_{pit}-E_{prot} show no temperature

dependence. This implies that the electrochemical repassivation of growing pits is temperature-insensitive in this environment.

Corrosion Rates

Tafel extrapolation and linear polarization resistance have been used to determine the corrosion rates of candidate steels under a variety of conditions. The rates determined by these methods are to be compared to those obtained by weight-loss measurements which were measured following 3548 and 5000 hr exposure periods in J-13 well water. The weight-loss data is given in Table 4. The data for three replicate samples has been averaged in the calculation of corrosion rates.

Typical plots for Tafel extrapolation and LPR for 316L in J-13 well water at 80°C are shown in Figs. 10 and 11, respectively. The plots were obtained and electrochemical corrosion rates determined with the aid of a PAR Model 350 Corrosion Measurement Console which is automatically controlled by an internal computer interface. The system automatically calculates a corrosion rate in terms of mils-per-year (mpy) from the measured corrosion current (I_{corr}). The system also calculates anodic and cathodic Tafel coefficients (ATC and CTC, respectively) which are used in the LPR measurement to calculate a corrosion current. The corrosion current is measured directly in the Tafel extrapolation technique, and is determined by the intersection of the extrapolated linear anodic and cathodic Tafel lines.

Figure 12 shows corrosion rates determined by Tafel extrapolation and LPR for 304L in J-13 well water containing an additional 1000 ppm NaCl at various temperatures. A similar correlation between the two different types of electrochemical measurements is given in Fig. 13 which displays data for 304L in J-13 well water at 90°C containing different concentrations of NaCl.

Considering the difference in the electrochemical techniques, and the low corrosion rates measured, reasonably good agreement is obtained (well within an order of magnitude) for most of the alloys in most environments. One can see in Fig. 13 that there is a significant increase in corrosion rate in going from 75 to 1000 ppm NaCl and from 1000 to 30,000 ppm NaCl as might be expected given the jump in severity of the environment. In this figure, the LPR data appear to be more internally consistent as one would expect a large jump in the corrosion rate in going from 1000 to 30,000 ppm NaCl. The data obtained by Tafel extrapolation for 30,000 ppm NaCl is anomalous and is being re-examined.

The electrochemically measured corrosion rates (by Tafel extrapolation) for prospective canister materials in tuff-conditioned J-13 well water as a function of temperature are given in Fig. 14. The general trend for 304L, I-825 and 321 is to show an increased corrosion rate with temperature, as expected for austenitic stainless steels (2-4). However, the changes in corrosion rate with temperature are slight and one would be tempted to interpret the corrosion rate for all the alloys in J-13 to be generally effectively independent of temperature (in the temperature range surveyed), especially for 316L, 317L, and 347. As a result of the relatively benign environment of J-13 well water, this would not be a surprising result for the temperature range considered and the limitations of the measurement technique employed. One might consider the electrochemically measured rates to be a conservative upper bound. The relatively large corrosion rate for 316L at 70°C (although it is still low, 1 mpy = 1 inch in 1000 years) is anomalous and deserves reexamination.

The fact that the electrochemical measurements represent a conservative upper bound for corrosion rates is exemplified by comparison with the measured

corrosion rates obtained by weight-loss shown in Table 3. These rates are all very much lower than the electrochemically measured rates. This again is the result of the difficulty of measuring absolute corrosion rates in the relatively benign environment at hand by either weight-loss or electrochemical methods, and in the large differences in the methods used to determine the rates. Differences in initial surface preparation and cleaning procedures, as well as the fact that "fresh" surfaces were used in the electrochemical experiments also may account for some of the discrepancies. Normally, as a rule of thumb in corrosion measurements, if the corrosion rates were several mils-per-year, one would expect an order-of-magnitude agreement between the two techniques. As a result of such low corrosion rates in this system, reasonable agreement (although certainly not within an order of magnitude) is believed to be obtained here.

Following exposure to J-13 well water for various times, the candidate alloys were removed and the corrosion rates were determined electrochemically. The results of such a study following exposure for 100, 500, 1000, and 2500 hours at 90°C are shown in Fig. 15. There is no clear correlation of corrosion rate with time as determined by Tafel extrapolation for any of the alloys. This same result is found in the weight-loss data. Again, the benignity of the environment may account for this and the comments given above apply here also. By comparison with the 90°C data in Fig. 14, which was obtained using "fresh" unexposed samples, it is observed that following exposure to J-13 well water the corrosion rates are observed to decrease at all times for all alloys. This may be the result of the formation of a more protective passive film on the surface following exposure. It is also observed that the measured corrosion rates in Fig. 15 more nearly match those of weight-loss measurements given in Table 3 (in many cases an

"order-of-magnitude" agreement is obtained, especially when comparison is made between the 5000 hours weight-loss data and the longer of the exposure times for the electrochemical samples. This may be due to more similar conditions of the alloy surface for the two measurement techniques following exposure than was the case for the comparison with "fresh" samples given in Fig. 14. The values for 304L and 321 at 2500 hours in Fig. 15 are anomalous and will be reexamined.

Role of Oxide Films

The canisters are expected to experience a high-temperature air environment for a significant time period after emplacement. Temperatures of approximately 200 to 250°C at the canister surface for up to 50 years may be reached for spent fuel waste packages (1). In addition, during the in-can glass solidification process proposed for commercial and defense high-level wastes, canister surface temperatures as high as 580°C may be reached during the processing. Previous studies (13) have indicated that for 304L, a maximum sensitivity to pitting will occur following oxidation in dry air at 300°C. This pitting susceptibility results from a change in the semiconducting properties of the oxide film.

We have recently initiated studies to examine the role of thermally formed oxide films on stainless steels on the resultant pitting susceptibility in chloride media. Preliminary results suggest that oxide films formed on 304L in dry air at 650°C for 1 hour inhibit overall pitting in 1000 ppm Cl^- media at 90°C. That is, the overall current density achieved upon anodic polarization is lower at any given potential for the oxidized specimen relative to an unoxidized specimen. However, this is a measure of the overall pitting current density and does not account for the possibility that some pits may grow more rapidly than others. Therefore, the maximum pit depth for

the oxidized specimen may be equal to or exceed that for the unoxidized specimen. Further examination is in progress.

Once pitting has been initiated on the thermally oxidized specimen by scanning to positive potentials, if the scan is reversed to more negative potentials the resultant current densities are similar to those obtained on the unoxidized specimens. This means that the films are not self-healing and if penetration of aggressive Cl^- ion into the film is allowed, the beneficial effects of the film are permanently destroyed. Further work will be more fully documented in a later report.

Future Work

Among the topics which are currently under investigation, or planned for the near future are the following:

1. Examination is underway to determine the sensitivity of evaluated parameters, e.g., E_{corr}, E_{pit}, etc., to surface preparation and test procedures. In this regard, data reproducibility is being critiqued.

2. More sophisticated electrochemical techniques are being used to investigate the mechanisms of pit initiation. In addition, surface analytical techniques (e.g., Auger electron spectroscopy) are being used to investigate the role of alloying constituents in pit initiation and repassivation.

3. Mechanisms of crevice corrosion for candidate alloys are being investigated. This localized form of attack has not yet been well

explored for this program and may provide differentiation of candidate alloys with regard to suitability as canister materials.

4. Effects of radiolysis on the electrochemical corrosion properties of prospective canister materials are being evaluated. Both in-situ gamma field and ex-situ modeling experiments are planned for the near future.

5. The electrochemical corrosion behavior of 316 stainless steel containing low carbon (to avoid sensitization) and high nitrogen (for greater strength and increased localized corrosion resistance) is under investigation. This material has been proposed for use in piping in nuclear power plants (BWR) and may be a viable canister material.

Conclusions

1. J-13 well water is a relatively benign environment towards the candidate alloys 304L, 316L, 317L, 321, 347, and I-825. Electrochemical results, obtained from anodic polarization curves, indicate that spontaneous pitting of these materials should not occur for these alloys at temperatures up to 100°C in this environment.

2. The values of E_{corr} in J-13 well water for many of the prospective materials is relatively insensitive to temperature up to 90°C. E_{pit} values become slightly more negative with temperature. Values for $E_{pit}-E_{prot}$ show no systematic temperature dependence.

3. Concentration of J-13 well water to ten times the original concentrations of solute species does not appear to significantly affect the fundamental electrochemical corrosion behavior of 316L.

4. However, increase of the Cl^- ion concentration alone in J-13 well water, creates a more aggressive solution towards austenitic stainless steels which is indicated in the electrochemical corrosion test results. With increase in Cl^- concentration in J-13, E_{corr} and E_{pit} values get more negative and the alloy becomes more susceptible to pitting. This is in agreement with previous work on the effect of Cl^-.

5. The electrochemical techniques of Tafel extrapolation and linear polarization resistance to determine corrosion rates yield no clear dependence on temperature in J-13. That the corrosion rates are so low in this environment may account for the observed lack of temperature dependence. This result is obtained by both weight-loss and electrochemical measurements. When NaCl is purposely added to J-13, the electrochemically measured corrosion rates increase, particularly when more than 75 ppm NaCl is added.

6. When compared to corrosion rates measured by weight-loss in-situ, the electrochemically measured rates are always larger. This is particularly true when "fresh" unexposed surfaces are used in the electrochemical experiments. When the electrochemical samples are immersed in solution under the same conditions as the weight-loss samples, thereby generating similar surfaces (oxide films) the correlation is better (in some cases within an order of magnitude). The electrochemically measured rates should be taken as conservative upper bounds.

7. On the basis of weight-loss measurements and electrochemical experiments in J-13 well water at temperatures up to 100°C it is not possible to definitively distinguish the behavior of 304L, 316L, 317L, 321, 347, or I-825 as to which is a more suitable canister material. All of these candidate materials exhibit sufficiently low corrosion rates and no indication of spontaneous pitting. Present experimental results indicate that a canister fabricated from any one of these candidate alloys could meet the 300-1000 year containment objective. However, due to the possible long-term low-temperature sensitization of 304L (14), 316L or one of the stabilized grades of steel may be preferable canister materials. Crevice corrosion is a form of attack to which many stainless alloys show some degree of susceptiblity and the performance of the candidate alloys may provide a means of differentiating between them in J-13 well water. Future work will be directed toward more sophisticated testing to differentiate the crevice corrosion susceptibility of the candidate alloys.

Acknowledgments

The assistance of William F. Frey in performing some of the laboratory experiments is gratefully acknowledged.

REFERENCES

1. R. D. McCright, H. Weiss, M. C. Juhas, and R. W. Logan, UCRL-89988, Nov., 1983.
2. A. J. Sedricks, Corrosion of Stainless Steels, John Wiley and Sons, New York (1979).
3. H. H. Uhlig, Corrosion and Corrosion Control, Second Edition, John Wiley and Sons, Inc., New York (1971).
4. M. G. Fontana and N. D. Greene, Corrosion Engineering, McGraw-Hill, New York (1978).
5. L. L. Shreir, Corrosion, Vols. 1 and 2, Newnes-Butterworths, Boston (1979).
6. R. W. Staehle, B. F. Brown, J. Kruger, and A. Agrawal, eds., Localized Corrosion, part III, pp. 311-447, National Association of Corrosion Engineers, Houston (1974).
7. A. J. Bard and L. R. Faulkner, Electrochemical Methods, John Wiley and Sons, Inc., New York (1980).
8. J. O'M. Bockris and A.K.N. Reddy, Modern Electrochemistry, Vols. 1 and 2, Plenum Press, New York (1970).
9. B. C. Syrett, Corrosion, 33, 221 (1977).
10. B. E. Wilde in Localized Corrosion, op cit., p. 342.
11. S. Smialowska and M. Czachor in Localized Corrosion, op cit., p. 353.
12. S. Szklarska-Smialowska, ibid, pp. 312-341.
13. G. Bianchi, A. Cerguetti, F. Mazza, and S. Torchio in Localized Corrosion, op cit., p. 399.
14. M. J. Fox, "An Overview of Low-Temperature Sensitization," LLNL Contractors report UCRL-15619, Dec. 1983.
15. R. D. McCright, "General and Localized Corrosion Resistance of Austenitic Stainless Steels in J-13 Water," Lawrence Livermore National Laboratory Report (in preparation).

TABLE 1 Analysis of J-13 Water

(average of 6 samples, by OES-ICP and IC)

	ppm
Al	<0.020
As	<0.060
B	0.11 ± 0.01
Be	0.003
Cd	<0.003
Co	<0.003
Cu	<0.003
Fe	<0.004
Li	0.044 ± 0.001
Mn	<0.0005
Mo	0.013 ± 0.002
Ni	<0.008
P	<0.124
Pb	0.022 ± 0.003
Se	<0.100
Si	27.0 ± 0.1
Sr	0.054 ± 0.005
U	<0.084
V	0.011 ± 0.001
Zn	<0.008
Ca	13.0 ± 0.1
K^+	5.5 ± 0.3
Mg	1.92 ± 0.01
Na	43.4 ± 0.3
Cl	7.1 ± 0.3
F	2.4 ± 0.1
NO_3^-	9.1 ± 0.2
$SO_4^=$	18.5 ± 0.1
HCO_3^-	132 ± 6

TABLE 2 Alloy Composition for Reference and Alternative Canister and Overpack Materials

Common Alloy Designations	UNS* Designations	Chemical Composition (weight per cent) Carbon (max.)	Manganese (max.)	Phosphorus (max.)	Sulfur (max.)	Silicon (max.)	Chromium (range)	Nickel (range)	Other Elements
304L	S30403	0.030	2.00	0.045	0.030	1.00	18.00-20.00	8.00-12.00	N: 0.10 max
316L	S31603	0.030	2.00	0.045	0.030	1.00	16.00-18.00	10.00-14.00	Mo: 2.00-3.00 N: 0.10 max
321	S31200	0.08	2.00	0.045	0.030	1.00	17.00-19.00	9.00-12.00	Ti: 5 x C min
825	N08825	0.05	1.0	not specified	0.03	0.5	19.5-23.5	38.0-46.0	Mo: 2.5-3.5 Ti: 0.6-1.2 Cu: 1.5-3.0 Al: 0.2 max

(Information adapted f~ ASTM specifications A-167, B-424, refer to ASTM Annual Book of Standards, ASTM, Philidelphia (1982)

Note: Other stainless alloys mentioned in text: 317L is similar to 316L but with the Mo content increased to 3.00-4.00 and the Cr levels adjusted to 18.00-20.00 and the Ni levels to 11.00-15.00. 347 is a niobium stabilized stainless steel otherwise similar to 321. Nb content is specified as 10 x C content.

* Unified Number System for Metals and Alloys. Society of Automotive Engineers, Inc. Publication SAE HSIU86a, Warrendale, PA (1977).

TABLE 3 Actual Compositions of Alloys
Wt %

Alloy	C	Mn	P	S	Si	Cr	Ni	Mo	Cu	N	Other
304L	0.023	1.76	0.026	0.006	0.54	18.12	11.47	0.18	0.24	0.050	bal-Fe
316L	0.015	1.63	0.032	0.028	0.33	16.52	10.42	2.17	0.20	0.058	bal-Fe
317L	0.019	1.83	0.033	0.026	0.54	18.37	13.64	3.18	--	0.074	bal-Fe
321	0.026	1.75	0.019	0.010	0.58	17.220	9.34	0.23	0.23	0.017	Ti 0.45 Co 0.110 bal-Fe
347	0.063	1.49	0.022	0.004	0.51	17.19	9.30	0.290	0.180	--	Co 0.030 Ta 0.006 Nb 0.794 bal-Fe
825	0.015	0.79	--	0.006	0.26	20.65	39.85	2.73	1.93	--	Fe 32.8 Ti 0.69

TABLE 4 Corrosion Rates of Candidate Stainless Steels in J-13 Water as Determined from Weight-Loss Data.

Alloy	Test Duration (hours)	Corrosion Rate, mpy Temperature (°C) 50	70	80	90	100
304L	3548	0.001	0.008	0.008	0.006	0.004
	5000	0.009	0.008	0.009	0.006	0.005
316L	3548	0.009	0.010	0.011	0.006	0.007
	5000	0.004	0.009	0.010	0.010	0.008
317L	3548	0.014	0.011	0.011	0.007	0.003
	5000	0.001	0.010	0.008	0.011	0.004
321	3548	0.007	0.012	0.008	0.008	0.003
	5000	0.005	0.011	0.008	0.013	0.001
347	3548	0.009	0.015	0.010	0.008	0.010
	5000	0.011	0.013	0.010	0.011	0.042
I-825	3548	0.012	0.011	0.007	0.008	0.006
	5000	0.015	0.009	0.008	0.011	0.011

To express corrosion rates in μm/yr, use the conversion factor 0.001 mpy = 0.025 μm/yr

Figure 1. Potentiodynamic anodic polarization curve for 304L in J-13 well water at 90°C. Scan rate was 1 mV/s. Scan starts from E_{corr}.

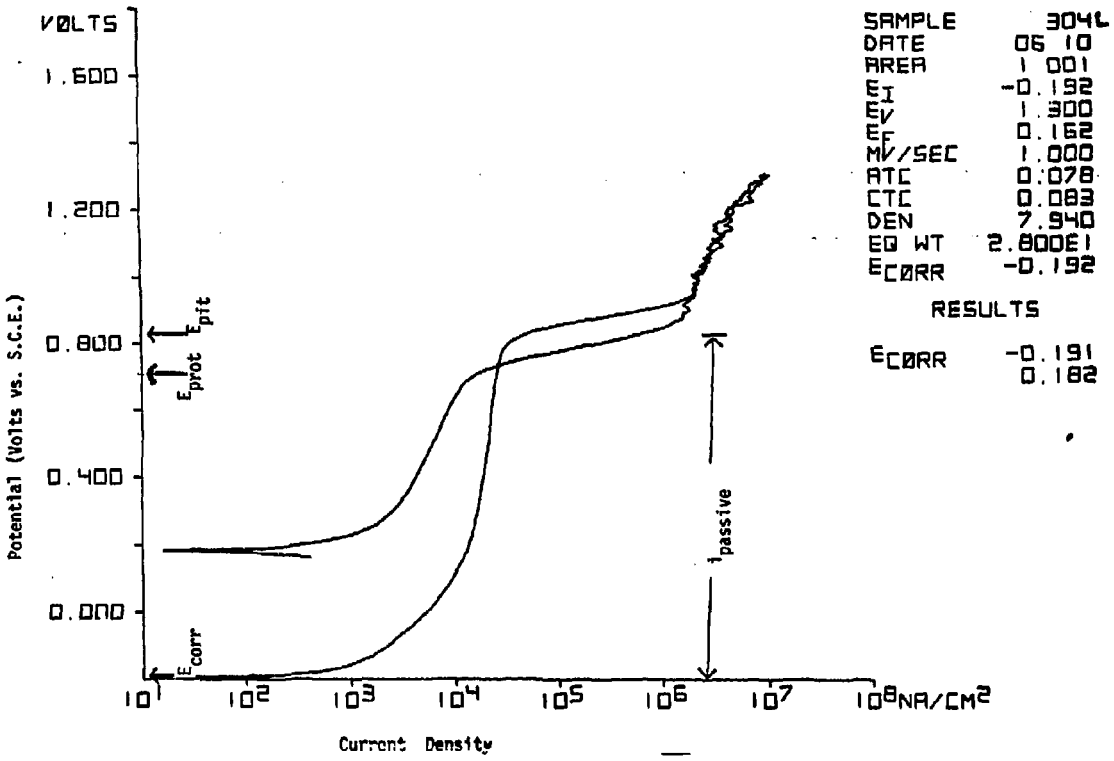

Figure 2. Electrochemical parameters for 304L in tuff-conditioned J-13 well water as a function of temperature. All potentials are referenced to an S.C.E. at 25°C.

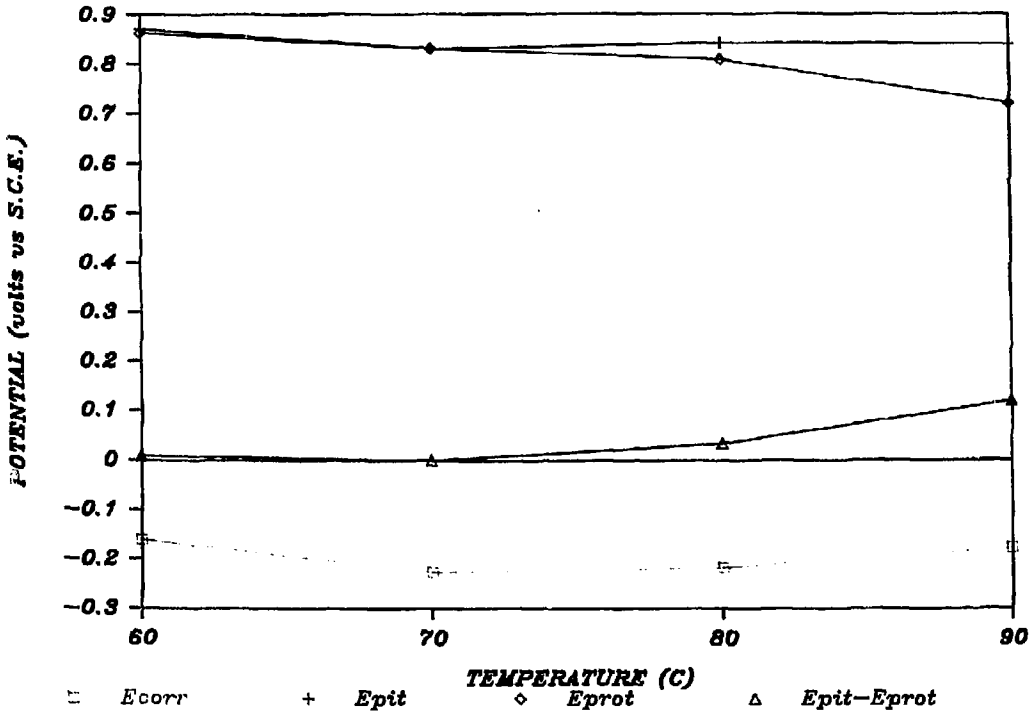

Figure 3. Electrochemical parameters for 316L analogous to those of figure 2 for 304L.

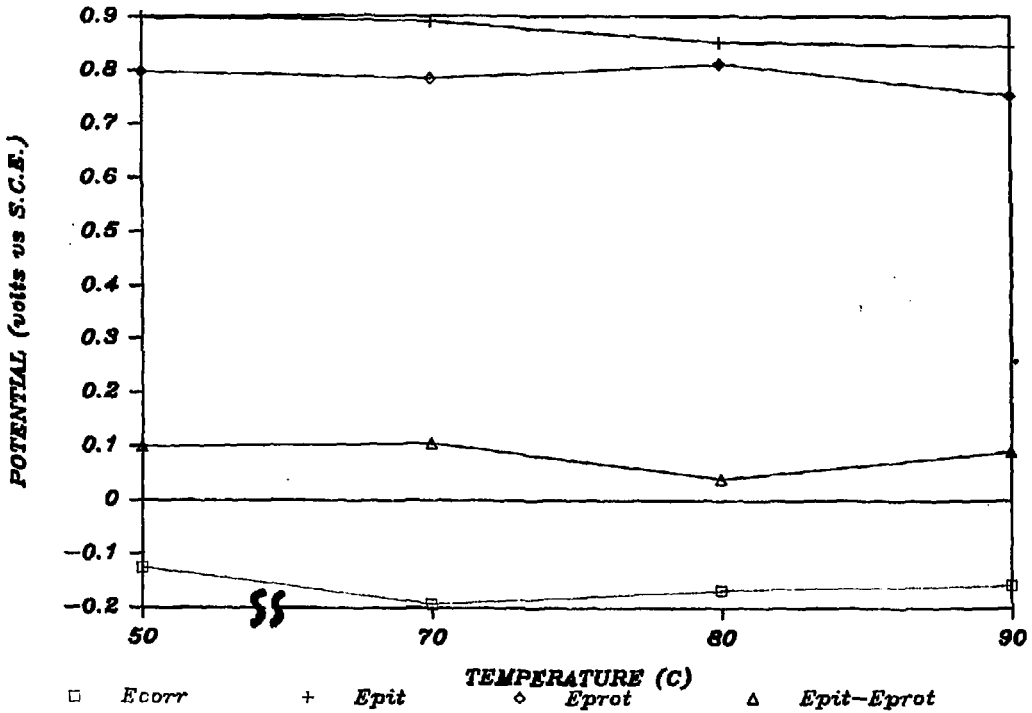

Figure 4. Electrochemical parameters for 1-825 analogous to those of figure 2 for 304L.

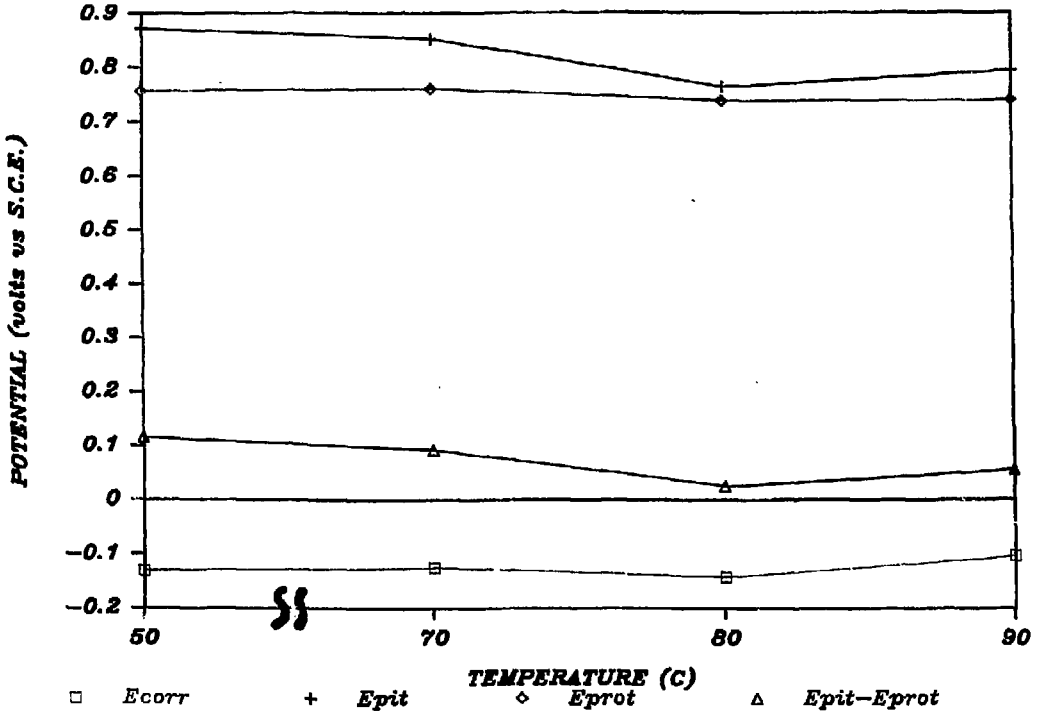

Figure 5. Potentiodynamic anodic polarization curve for 316L in deaerated J-13 well water with added 100 ppm Cl^- at 90°C. Scan rate was 1 mV/s and started from E_{corr}.

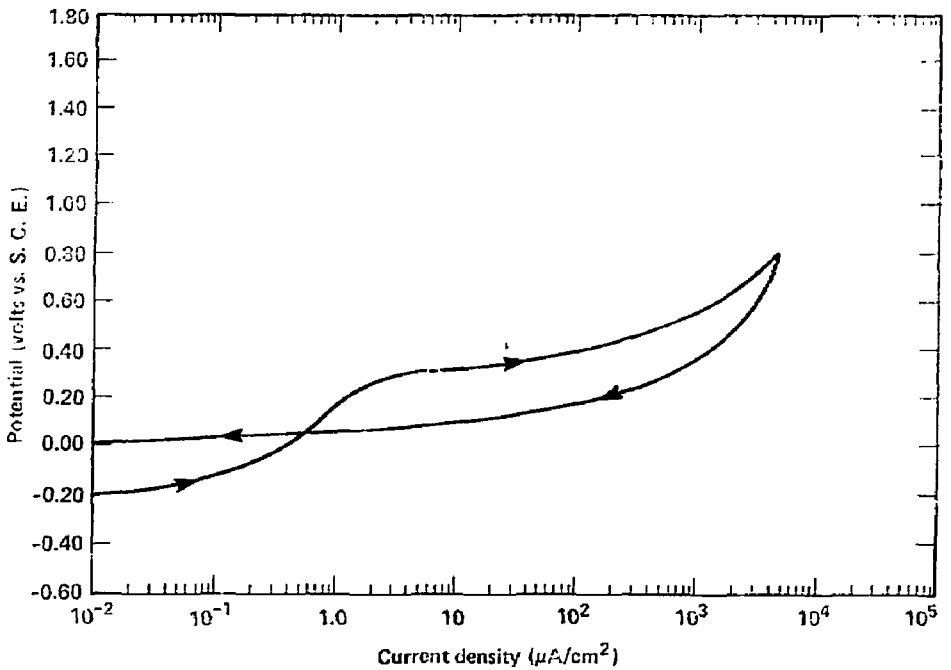

Figure 6. As for figure 5 only with an added 1000 ppm Cl^-.

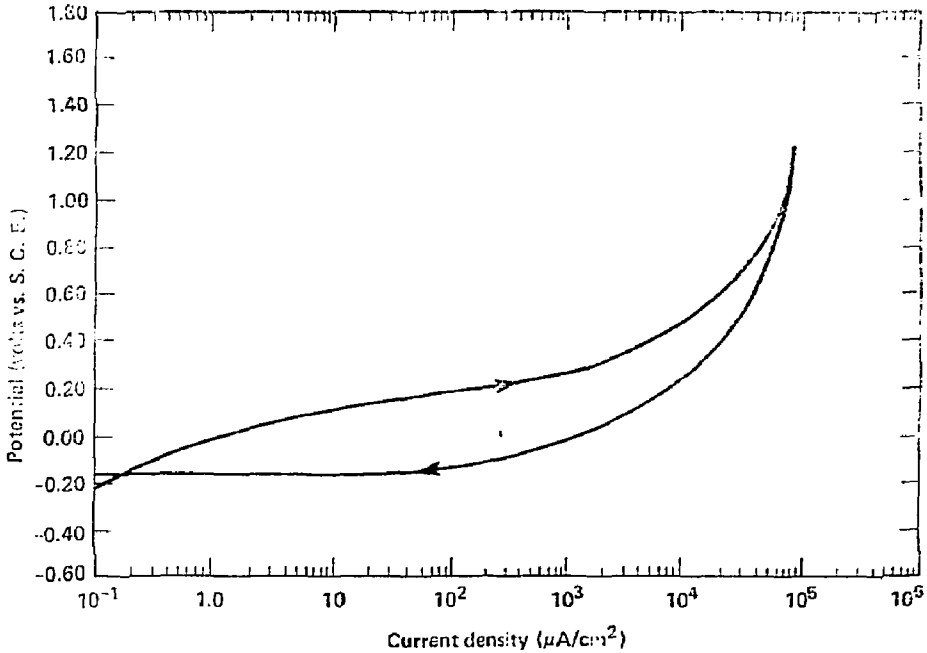

Figure 7. Values of E_{corr} and E_{pit} for 304L in tuff-conditioned J-13 well water with different concentrations of NaCl at 90°C.

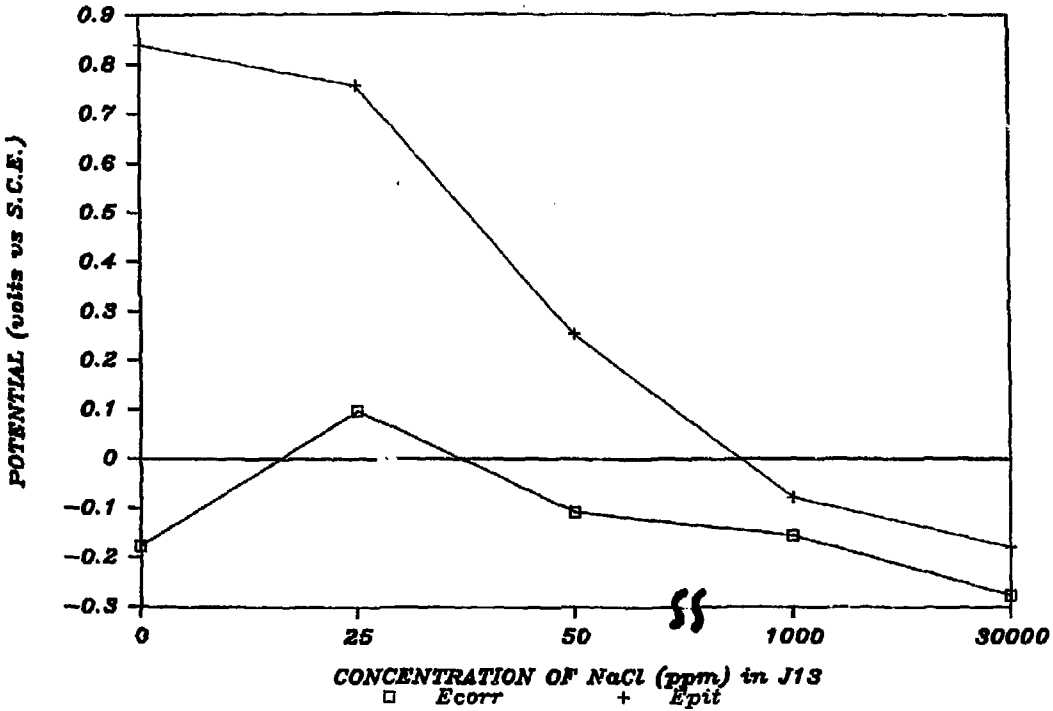

Figure 8. Values of E_{corr} and E_{pit} as a function of temperature for 304L in tuff-conditioned J-13 well water to which 75 ppm NaCl has been added.

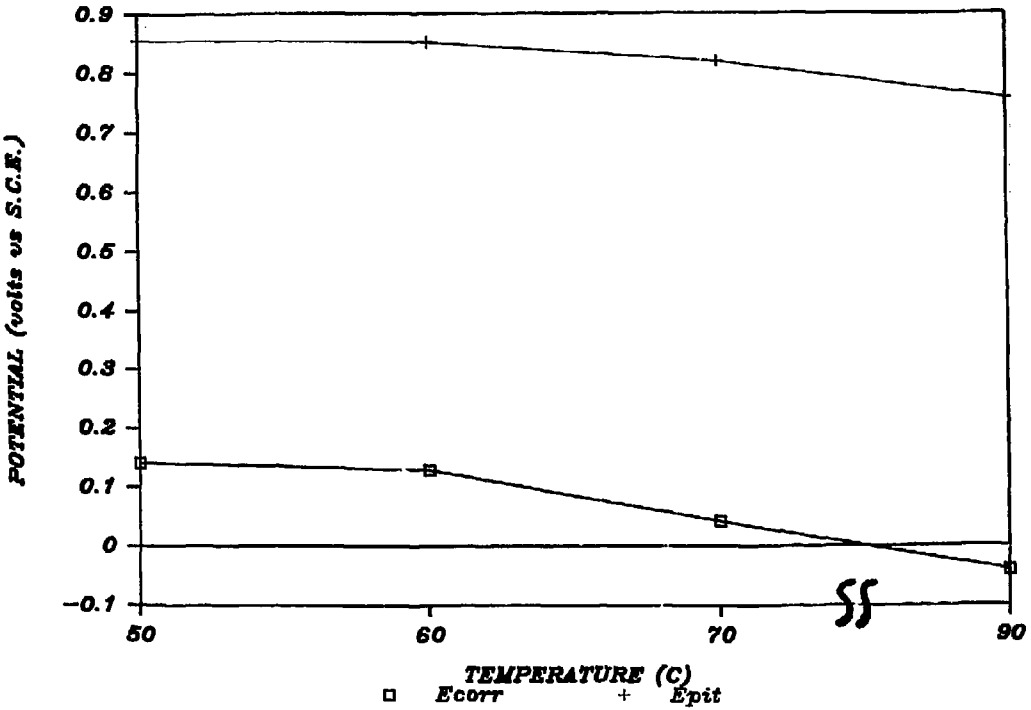

Figure 9. Electrochemical parameters for 304L as a function of temperature in tuff-conditioned J-13 well water to which 1000 ppm NaCl has been added.

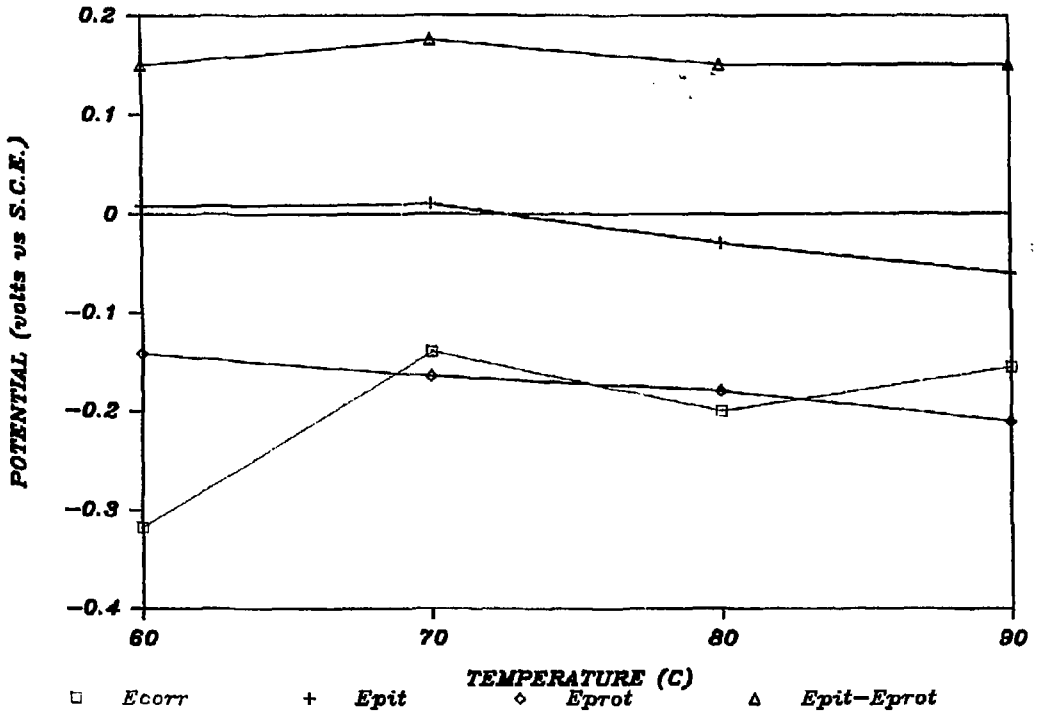

Figure 10. Example of the Tafel extrapolation method used to calculate the electrochemical corrosion rate. Plot shown is for 316L in tuff-conditioned J-13 well water at 80°C. The corrosion current is defined by the intersection of the linear anodic and cathodic Tafel lines.

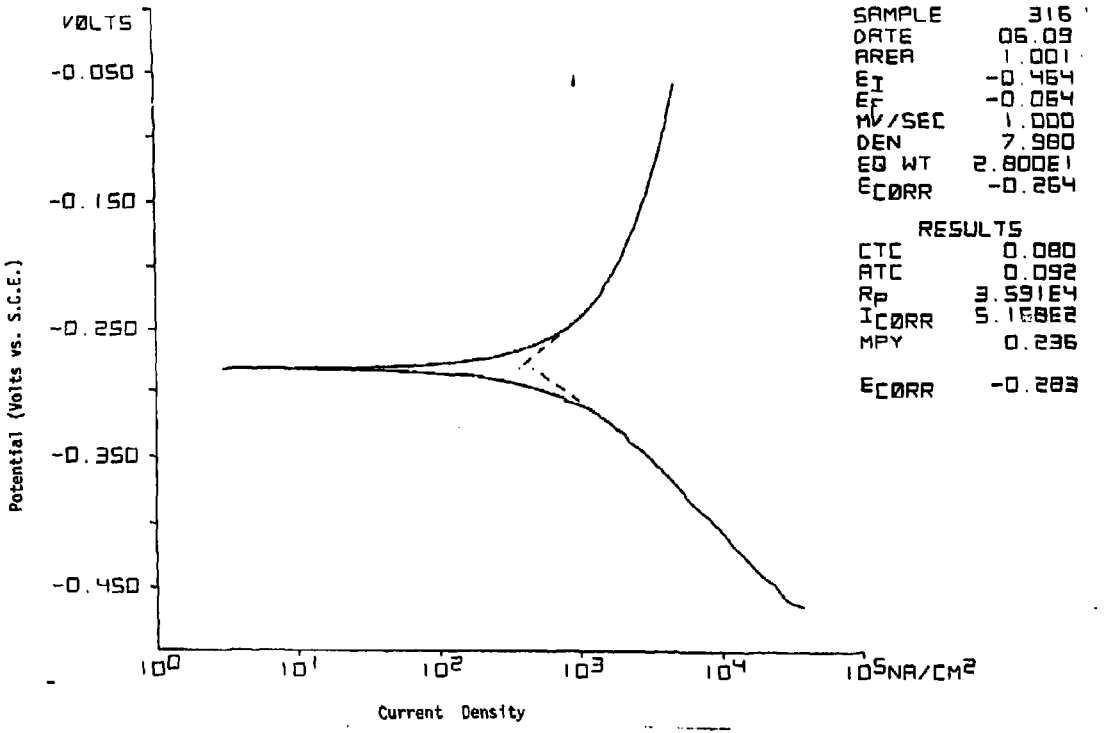

Figure 11. Example of the linear polarization resistance method used to obtain electrochemical corrosion rates. Conditions were the same as for figure 10. The linear segment of the curve generates a "polarization resistance" from which a corrosion rate can be calculated.

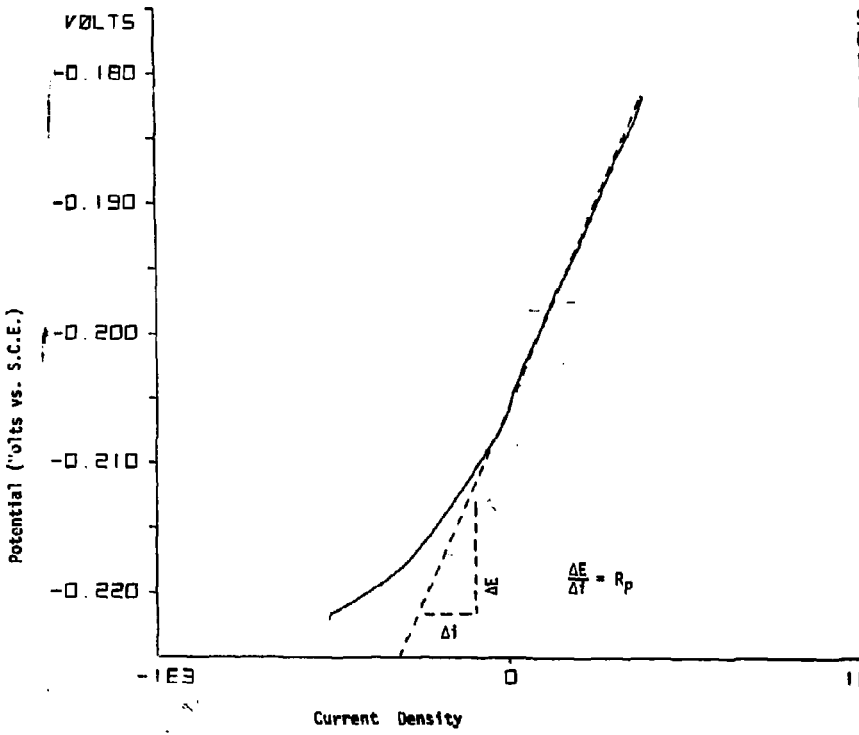

SAMPLE	316
DATE	06.09
AREA	1.001
E_I	-0.222
E_F	-0.182
MV/SEC	1.000
ATC	0.092
CTC	0.080
DEN	7.980
EQ WT	2.800E1
E_{CORR}	-0.202

RESULTS

R_P	6.154E4
I_{CORR}	3.020E2
MPY	0.138
E_{CORR}	-0.206

Figure 12. Plot of the electrochemical corrosion rates as determined both from Tafel extrapolation and linear polarization resistance for 304L in tuff-conditioned J-13 well water with an added 1000 ppm NaCl.

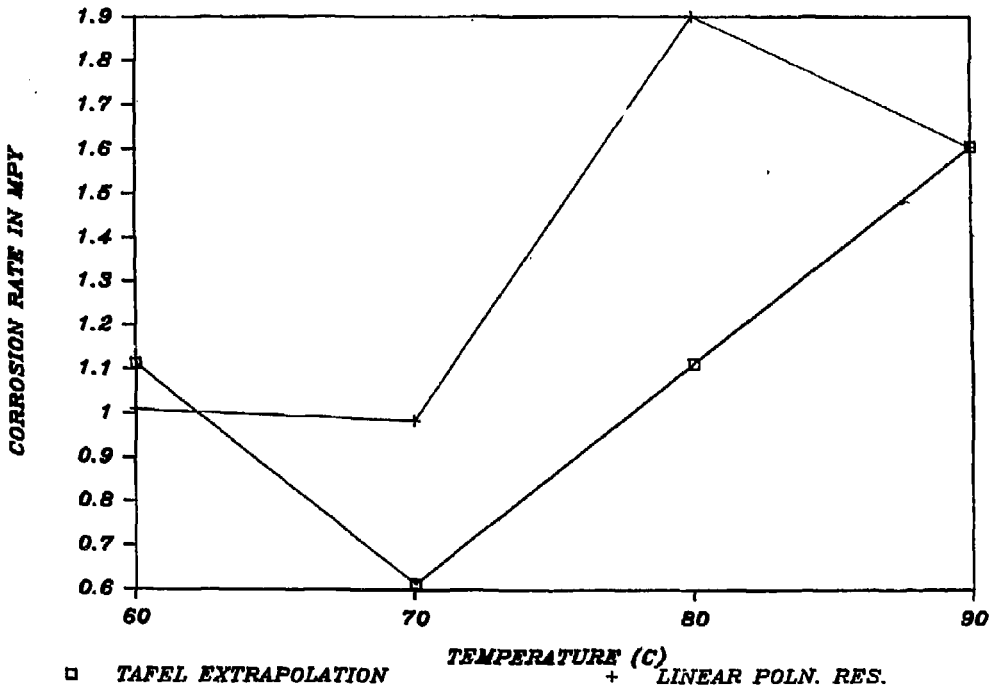

Figure 13. Electrochemical corrosion rates for 304L in tuff-conditioned J-13 well water at 90°C with different concentrations of added NaCl.

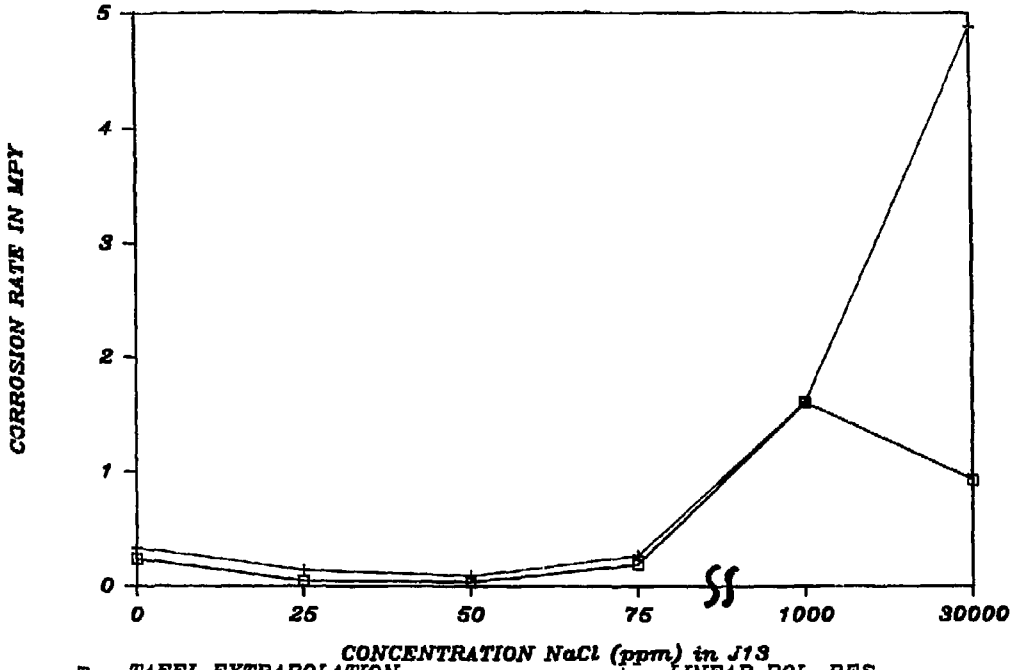

Figure 14. Corrosion rates for candidate alloys in tuff-conditioned J-13 well water at different temperatures. The Tafel extrapolation method was used.

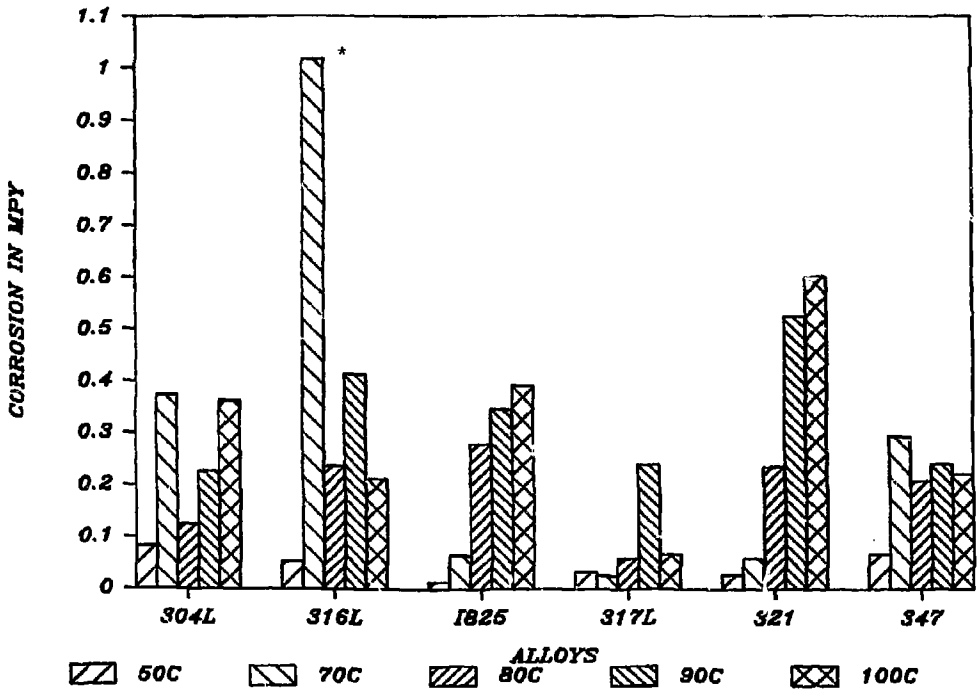

* In relation to the other values, this value appears anomalously high. See discussion on page 13.

Figure 15. Electrochemical corrosion rates for candidate alloys in tuff-conditioned J-13 at 90°C following different times of exposure. Tafel extrapolation was used.